J. Fluid Mech. (2010), *vol.* 649, *pp.* 329–340.
doi:10.1017/S0022112010000224

Transient flow of a viscous compressible fluid in a circular tube after a sudden point impulse transverse to the axis

B. U. FELDERHOF†

Institut für Theoretische Physik A, RWTH Aachen University, Templergraben 55, 52056 Aachen, Germany

(Received 19 October 2009; revised 7 January 2010; accepted 10 January 2010)

The flow of a viscous compressible fluid in a circular tube generated by a sudden impulse at a point on the axis and directed transverse to the axis is studied on the basis of the linearized Navier–Stokes equations. A no-slip boundary condition is assumed to hold on the wall of the tube. The flow behaviour differs qualitatively from that for a point impulse in the direction of the axis in that there is no coupling to a diffusive sound mode. As a consequence, the transverse velocity autocorrelation function of a suspended Brownian particle decays at long times faster than $t^{-3/2}$.

1. Introduction

In a previous paper (Felderhof 2009), we have studied the flow dynamics of a viscous compressible fluid in a circular tube after a sudden impulse at a point on the axis and directed along the axis. It was shown that compressibility has a strong effect on the flow in confined geometry. In particular, the flow velocity at the source point shows an algebraic $t^{-3/2}$ long-time tail with amplitude proportional to the square root of the compressibility. The effect was demonstrated in computer simulation by Hagen *et al.* (1997). It was shown by Pagonabarraga *et al.* (1999) that the long-time tail is due to the coupling to diffusive sound modes of long wavelength.

In the following, we study the dynamics of flow in a circular tube generated by a sudden point impulse on the axis of the tube and directed transverse to the axis. The analysis is based on the solution of the linearized Navier–Stokes equations for a compressible viscous fluid. The explicit form of the corresponding Green function is found as an integral over wavenumber and frequency. The time dependence of the flow is again strongly affected by compressibility, but in the present geometry the velocity does not show a $t^{-3/2}$ long-time tail.

In the limit of zero frequency, compressibility plays no role. Therefore, the integral of the Green function over all time is identical to the steady-state Green function studied by Hasimoto (1976) and Liron & Shahar (1978) for an incompressible fluid. Because of the choice of source point on the axis, the present solution takes a simpler form than the one for general choice of source point studied by these authors. For transverse excitation the steady-state pressure disturbance decays rapidly with distance along the tube axis, in contrast to the case of parallel excitation, where there is a non-vanishing pressure drop between both ends of the tube.

† Email address for correspondence: ufelder@physik.rwth-aachen.de

The velocity autocorrelation function of a suspended Brownian particle, initially located on the axis, may be obtained from the present calculation in the approximation where the particle size is neglected. The calculation shows that the correlation function of the transverse velocity after a short time changes sign and tends to zero with a rapidly decaying negative long-time tail. This result differs qualitatively from that for plane plate geometry found in lattice Boltzmann computer simulation by Frydel & Rice (2006, 2007). These authors found a positive decay with superposed oscillations at long times because of sound bouncing from the plates, both for no-slip and perfect slip boundary conditions at the plates. The different behaviour must be due to the difference in geometry.

2. Linear hydrodynamics of flow in a circular tube

We consider a viscous compressible fluid of shear viscosity η, bulk viscosity η_v and equilibrium mass density ρ_0 located in a circular tube of radius b. We choose coordinates such that the z axis is along the axis of the tube and use cylindrical coordinates (R, φ, z). For time $t < 0$, the fluid is at rest at the static pressure p_s. At time $t = 0$, an impulse $\boldsymbol{P}$ is imparted to the fluid at the origin and directed along the x axis. We study the resulting motion of the fluid for time $t > 0$.

For small-amplitude motion, the flow velocity $\boldsymbol{v}(\boldsymbol{r}, t)$ and the pressure $p(\boldsymbol{r}, t)$ are governed by the linearized Navier–Stokes equations

$$\left.\begin{aligned} \rho_0 \frac{\partial \boldsymbol{v}}{\partial t} &= \eta \nabla^2 \boldsymbol{v} + \left(\frac{1}{3}\eta + \eta_v\right) \nabla\nabla \cdot \boldsymbol{v} - \nabla p + \boldsymbol{P}\delta(\boldsymbol{r})\delta(t), \\ \frac{\partial p}{\partial t} &= -\rho_0 c_0^2 \nabla \cdot \boldsymbol{v}, \end{aligned}\right\} \tag{2.1}$$

with impulse $\boldsymbol{P} = P\boldsymbol{e}_x$ and long-wave sound velocity c_0. We assume that the flow velocity satisfies the no-slip boundary condition at the wall of the cylinder, i.e. $\boldsymbol{v} = \boldsymbol{0}$ at $R = b$. We look for the solution of (2.1) for which the flow velocity $\boldsymbol{v}(\boldsymbol{r}, t)$ vanishes and the pressure tends to the static pressure p_s as $z \to \pm\infty$ at any time t.

After Fourier analysis in time, we find that the equations for the Fourier components

$$\boldsymbol{v}_\omega(\boldsymbol{r}) = \int_0^\infty \mathrm{e}^{\mathrm{i}\omega t} \boldsymbol{v}(\boldsymbol{r}, t)\, \mathrm{d}t, \qquad p_\omega(\boldsymbol{r}) = \int_0^\infty \mathrm{e}^{\mathrm{i}\omega t} [p(\boldsymbol{r}, t) - p_s]\, \mathrm{d}t \tag{2.2}$$

are

$$\left.\begin{aligned} \eta\left(\nabla^2 \boldsymbol{v}_\omega - \alpha^2 \boldsymbol{v}_\omega\right) + \left(\frac{1}{3}\eta + \eta_v\right) \nabla\nabla \cdot \boldsymbol{v}_\omega - \nabla p_\omega &= -\boldsymbol{P}\delta(\boldsymbol{r}), \\ \nabla \cdot \boldsymbol{v}_\omega - \mathrm{i}\beta p_\omega &= 0, \end{aligned}\right\} \tag{2.3}$$

where we have used the abbreviations

$$\alpha = \sqrt{\frac{-\mathrm{i}\omega\rho_0}{\eta}}, \qquad \mathrm{Re}\,\alpha > 0, \qquad \beta = \frac{\omega}{\rho_0 c_0^2}. \tag{2.4}$$

We write the Fourier-transformed flow velocity as

$$\boldsymbol{v}_\omega(\boldsymbol{r}) = \boldsymbol{v}_{0\omega}(\boldsymbol{r}) + \boldsymbol{v}_{1\omega}(\boldsymbol{r}), \tag{2.5}$$

where $\boldsymbol{v}_{0\omega}(\boldsymbol{r})$ is the solution for infinite space and $\boldsymbol{v}_{1\omega}(\boldsymbol{r})$ is the reflected flow because of the presence of the boundary. The flows can be expressed as

$$\boldsymbol{v}_{0\omega}(\boldsymbol{r}) = \mathsf{G}_0(\boldsymbol{r} - \boldsymbol{r}_0) \cdot \boldsymbol{P}, \qquad \boldsymbol{v}_\omega(\boldsymbol{r}) = \mathsf{G}(\boldsymbol{r}, \boldsymbol{r}_0) \cdot \boldsymbol{P}, \tag{2.6}$$

with Green functions G_0 and G. The Green function for infinite space is translationally invariant and given explicitly by (Jones 1981)

$$G_0(\boldsymbol{r}) = \frac{1}{4\pi\eta}\left(\frac{\mathrm{e}^{-\alpha r}}{r}\mathbf{1} + \alpha^{-2}\nabla\nabla\frac{\mathrm{e}^{\mathrm{i}\mu r} - \mathrm{e}^{-\alpha r}}{r}\right), \tag{2.7}$$

with the abbreviation

$$\mu = \omega/c, \qquad \mathrm{Im}\mu > 0, \tag{2.8}$$

where

$$c = c_0\left[1 - \mathrm{i}\beta\left(\frac{4}{3}\eta + \eta_v\right)\right]^{1/2}. \tag{2.9}$$

It is convenient to use complex notation and consider the initial impulse $\boldsymbol{P} = P(\boldsymbol{e}_x + \mathrm{i}\boldsymbol{e}_y)$. Then the flow velocity $\boldsymbol{v}_{0\omega}$ for infinite space can be expressed as

$$\left.\begin{aligned} v_{0R\omega}(\boldsymbol{r}) &= \frac{P}{2\pi^2\eta\alpha^2}\,\mathrm{e}^{\mathrm{i}\varphi}\int_0^\infty \hat{v}_{0R}(k,\omega,R)\cos kz\;\mathrm{d}k,\\ v_{0\varphi\omega}(\boldsymbol{r}) &= \frac{P}{2\pi^2\eta\alpha^2}\,\mathrm{e}^{\mathrm{i}\varphi}\int_0^\infty \hat{v}_{0\varphi}(k,\omega,R)\cos kz\;\mathrm{d}k,\\ v_{0z\omega}(\boldsymbol{r}) &= \frac{P}{2\pi^2\eta\alpha^2}\,\mathrm{e}^{\mathrm{i}\varphi}\int_0^\infty \hat{v}_{0z}(k,\omega,R)\sin kz\;\mathrm{d}k, \end{aligned}\right\} \tag{2.10}$$

with amplitudes

$$\left.\begin{aligned} \hat{v}_{0R}(k,\omega,R) &= -k^2K_0(sR) - \frac{s}{R}K_1(sR) + u^2K_0(uR) + \frac{u}{R}K_1(uR),\\ \hat{v}_{0\varphi}(k,\omega,R) &= i\alpha^2K_0(sR) + \mathrm{i}\frac{s}{R}K_1(sR) - \mathrm{i}\frac{u}{R}K_1(uR),\\ \hat{v}_{0z}(k,\omega,R) &= -ksK_1(sR) + kuK_1(uR), \end{aligned}\right\} \tag{2.11}$$

with modified Bessel functions $K_n(x)$ and the abbreviations

$$s = \sqrt{k^2 + \alpha^2}, \qquad u = \sqrt{k^2 - \mu^2}. \tag{2.12}$$

The above expressions are derived by differentiation of the fundamental identity

$$\frac{2}{\pi}\int_0^\infty K_0(\sqrt{k^2+\alpha^2}R)\cos kz\;\mathrm{d}k = \frac{\mathrm{e}^{-\alpha r}}{r}. \tag{2.13}$$

The latter follows from the fact that both right- and left-hand sides satisfy the Helmholtz equation for $r > 0$ and have the same singularity at $r = 0$ (see also Gradshteyn & Ryzhik 1965, expressions 6.726.4 and 8.469.3).

In analogy with (2.10) we write the reflected flow velocity $\boldsymbol{v}_{1\omega}$ as

$$\left.\begin{aligned} v_{1R\omega}(\boldsymbol{r}) &= \frac{P}{2\pi^2\eta\alpha^2}\,\mathrm{e}^{\mathrm{i}\varphi}\int_0^\infty \hat{v}_{1R}(k,\omega,R)\cos kz\;\mathrm{d}k,\\ v_{1\varphi\omega}(\boldsymbol{r}) &= \frac{P}{2\pi^2\eta\alpha^2}\,\mathrm{e}^{\mathrm{i}\varphi}\int_0^\infty \hat{v}_{1\varphi}(k,\omega,R)\cos kz\;\mathrm{d}k,\\ v_{1z\omega}(\boldsymbol{r}) &= \frac{P}{2\pi^2\eta\alpha^2}\,\mathrm{e}^{\mathrm{i}\varphi}\int_0^\infty \hat{v}_{1z}(k,\omega,R)\sin kz\;\mathrm{d}k, \end{aligned}\right\} \tag{2.14}$$

with amplitudes

$$\left.\begin{aligned}\hat{v}_{1R}(k,\omega,R) &= A(k,\omega)v_{Rp}(k,\omega,R) + B(k,\omega)v_{Rv}(k,\omega,R) + C(k,\omega)v_{Rs}(k,\omega,R),\\ \hat{v}_{1\varphi}(k,\omega,R) &= A(k,\omega)v_{\varphi p}(k,\omega,R) + B(k,\omega)v_{\varphi v}(k,\omega,R) + C(k,\omega)v_{\varphi s}(k,\omega,R),\\ \hat{v}_{1z}(k,\omega,R) &= A(k,\omega)v_{zp}(k,\omega,R) + B(k,\omega)v_{zv}(k,\omega,R) + C(k,\omega)v_{zs}(k,\omega,R),\end{aligned}\right\} \tag{2.15}$$

where

$$\left.\begin{aligned}&v_{Rp}(k,\omega,R) = -u^2 I_0(uR) + \frac{u}{R}I_1(uR), \qquad v_{\varphi p}(k,\omega,R) = -\mathrm{i}\frac{u}{R}I_1(uR),\\ &v_{zp}(k,\omega,R) = kuI_1(uR), \qquad v_{Rv}(k,\omega,R) = -k^2 I_0(sR) + \frac{s}{R}I_1(sR),\\ &v_{\varphi v}(k,\omega,R) = \mathrm{i}\alpha^2 I_0(sR) - \mathrm{i}\frac{s}{R}I_1(sR), \qquad v_{zv}(k,\omega R) = ksI_1(sR),\\ &v_{Rs}(k,\omega,R) = \frac{1}{R}I_1(sR), \qquad v_{\varphi s}(k,\omega,R) = \mathrm{i}sI_0(sR) - \frac{\mathrm{i}}{R}I_1(sR),\\ &v_{zs}(k,\omega R) = 0,\end{aligned}\right\} \tag{2.16}$$

with modified Bessel functions $I_n(x)$. Together with the expression for the pressure given in (2.22), the expressions in (2.14) provide the general solution to (2.3) which is regular everywhere, except infinity, and is symmetric in z. This must be combined with the singular solution given by (2.10), (2.11) and (2.21). From the no-slip boundary condition at $R = b$, we find for the coefficients $A(k,\omega)$, $B(k,\omega)$ and $C(k,\omega)$:

$$A(k,\omega) = \frac{P(k,\omega)}{Z(k,\omega)}, \qquad B(k,\omega) = \frac{Q(k,\omega)}{Z(k,\omega)}, \qquad C(k,\omega) = \frac{S(k,\omega)}{Z(k,\omega)} \tag{2.17}$$

with denominator

$$\begin{aligned}Z(k,\omega) = {} & suI_0(ub)I_1(sb)^2 + k^2 sbI_0(sb)^2 I_1(ub)\\ & + I_0(sb)I_1(sb)\big[(s^2 - 2k^2)I_1(ub) - s^2 ubI_0(ub)\big]\end{aligned} \tag{2.18}$$

and numerators

$$\left.\begin{aligned}P(k,\omega) = {} & \frac{1}{u}[sI_1(sb)^2((s^2 - 2k^2)K_0(sb) + u^2 K_0(ub)) + k^2 sbI_0(sb)^2(sK_1(sb)\\ & - uK_1(ub)) + I_0(sb)I_1(sb)(k^2 s^2 bK_0(sb) - s^2 u^2 bK_0(ub)\\ & + (s^2 - 2k^2)(sK_1(sb) - uK_1(ub)))],\\ Q(k,\omega) = {} & -sbI_0(sb)[I_1(ub)(k^2 K_0(sb) - u^2 K_0(ub))\\ & + uI_0(ub)(sK_1(sb) - uK_1(ub))] - I_1(sb)[I_1(ub)((s^2 - 2k^2)K_0(sb)\\ & + u^2 K_0(ub)) - uI_0(ub)(sK_1(sb) - uK_1(ub))],\\ S(k,\omega) = {} & -\alpha^2 u[I_0(sb) - I_0(ub)].\end{aligned}\right\} \tag{2.19}$$

The Fourier transform of the pressure corresponding to the point excitation in infinite space takes the form

$$p_{0\omega}(\boldsymbol{r}) = \frac{P}{4\pi}\frac{c_0^2}{c^2}\frac{Re^{\mathrm{i}\varphi}}{r^3}(1 - \mathrm{i}\mu r)\mathrm{e}^{\mathrm{i}\mu r}. \tag{2.20}$$

This can be cast in the alternative form

$$p_{0\omega}(\boldsymbol{r}) = \frac{P}{2\pi^2}\frac{c_0^2}{c^2}\,\mathrm{e}^{\mathrm{i}\varphi}\int_0^\infty uK_1(uR)\cos kz\;\mathrm{d}k. \tag{2.21}$$

The pressure corresponding to the reflected flow field given by (2.14) is

$$p_{1\omega}(\boldsymbol{r}) = \frac{P}{2\pi^2}\frac{c_0^2}{c^2}\,\mathrm{e}^{\mathrm{i}\varphi}\int_0^\infty A(k,\omega)uI_1(uR)\cos kz\;\mathrm{d}k. \tag{2.22}$$

It is evident from (2.3) that in the limit of zero frequency, the equations reduce to the steady-state Stokes equations for an incompressible fluid. Hence, the integral over all time of the velocity field $\boldsymbol{v}(\boldsymbol{r},t)$ and the pressure disturbance $p(\boldsymbol{r},t)-p_s$ must be identical to the expressions found by Hasimoto (1976) and Liron & Shahar (1978).

3. Steady-state limit

It is worthwhile to consider separately the steady-state limit of the above expressions, corresponding to zero frequency. The calculation yields the Green function for the steady-state Stokes equations for source point at the origin and no-slip boundary condition at the wall of the cylinder. The Green function for arbitrary source point has been obtained earlier directly from the Stokes equations (Hasimoto 1976; Liron & Shahar 1978; Ishii & Hasimoto 1980).

We consider first the Green function for infinite space. From (2.10) and (2.11) we find at zero frequency

$$\left.\begin{aligned} v_{0R0}(\boldsymbol{r}) &= \frac{P}{4\pi^2\eta}\,\mathrm{e}^{\mathrm{i}\varphi}\int_0^\infty \left[K_0(kR)+kRK_1(kR)\right]\cos kz\;\mathrm{d}k = \frac{P}{8\pi\eta}\frac{R^2+r^2}{r^3}\mathrm{e}^{\mathrm{i}\varphi},\\ v_{0\varphi0}(\boldsymbol{r}) &= \frac{P}{4\pi^2\eta}\,\mathrm{i}\mathrm{e}^{\mathrm{i}\varphi}\int_0^\infty K_0(kR)\cos kz\;\mathrm{d}k = \frac{P}{8\pi\eta}\frac{\mathrm{i}\mathrm{e}^{\mathrm{i}\varphi}}{r},\\ v_{0z0}(\boldsymbol{r}) &= \frac{P}{4\pi^2\eta}\,\mathrm{e}^{\mathrm{i}\varphi}\int_0^\infty kRK_0(kR)\sin kz\;\mathrm{d}k = \frac{P}{8\pi\eta}\frac{(x+\mathrm{i}y)z}{r^3}, \end{aligned}\right\} \tag{3.1}$$

in agreement with Oseen's tensor. The corresponding pressure is found from (2.21) as

$$p_{00}(\boldsymbol{r}) = \frac{P}{2\pi^2}\,\mathrm{e}^{\mathrm{i}\varphi}\int_0^\infty kK_1(kR)\cos kz\;\mathrm{d}k = \frac{P}{4\pi}\frac{x+\mathrm{i}y}{r^3}. \tag{3.2}$$

It is less straightforward to take the zero frequency limit in (2.14). We write the resulting expressions as

$$\left.\begin{aligned} v_{1R0}(\boldsymbol{r}) &= \frac{P}{2\pi^2\eta}\,\mathrm{e}^{\mathrm{i}\varphi}\int_0^\infty u_{1R}(k,R)\cos kz\;\mathrm{d}k,\\ v_{1\varphi0}(\boldsymbol{r}) &= \frac{P}{2\pi^2\eta}\,\mathrm{e}^{\mathrm{i}\varphi}\int_0^\infty u_{1\varphi}(k,R)\cos kz\;\mathrm{d}k,\\ v_{1z0}(\boldsymbol{r}) &= \frac{P}{2\pi^2\eta}\,\mathrm{e}^{\mathrm{i}\varphi}\int_0^\infty u_{1z}(k,R)\sin kz\;\mathrm{d}k. \end{aligned}\right\} \tag{3.3}$$

The amplitudes $u_{1R}(k, R)$, $u_{1\varphi}(k, R)$ and $u_{1z}(k, R)$ can be expressed as

$$\left.\begin{aligned} u_{1R}(k, R) &= A_0(k)I_0(kR) + A_1(k)\frac{bI_1(kR)}{R} + A_2(k)kRI_1(kR), \\ u_{1\varphi}(k, R) &= B_0(k)I_0(kR) + B_1(k)\frac{bI_1(kR)}{R}, \\ u_{1z}(k, R) &= C_0(k)kRI_0(kR) + C_1(k)I_1(kR) \end{aligned}\right\} \tag{3.4}$$

with coefficients

$$\left.\begin{aligned} A_0(k) &= \frac{P_0(kb)}{M(kb)}, \qquad A_1(k) = \frac{P_1(kb)}{M(kb)}, \qquad A_2(k) = \frac{P_2(kb)}{M(kb)}, \\ B_0(k) &= \frac{Q_0(kb)}{M(kb)}, \qquad B_1(k) = \frac{Q_1(kb)}{M(kb)}, \\ C_0(k) &= \frac{S_0(kb)}{M(kb)}, \qquad C_1(k) = \frac{S_1(kb)}{M(kb)} \end{aligned}\right\} \tag{3.5}$$

with denominator

$$M(q) = 2[q^2I_0(q)^3 - qI_0(q)^2I_1(q) - (2+q^2)I_0(q)I_1(q)^2 + qI_1(q)^3] \tag{3.6}$$

and numerators

$$\left.\begin{aligned} P_0(q) &= qI_0(q)I_1(q)K_0(q) - q^2I_0(q)^2K_0(q) + (2+q^2)I_1(q)^2K_0(q) \\ &\quad + qI_1(q)^2K_1(q) - q^2I_0(q), \; P_1(q) = qI_0(q) + I_1(q), \\ P_2(q) &= -P_0(q) - q^2I_0(q) + qI_1(q), \\ Q_0(q) &= \mathrm{i}P_0(q) + \mathrm{i}qP_1(q), \qquad Q_1(q) = -\mathrm{i}P_1(q), \\ S_0(q) &= -P_2(q), \qquad S_1(q) = q^2I_0(q) - qI_1(q). \end{aligned}\right\} \tag{3.7}$$

Although the expressions are complicated, they are much simpler than those of Ishii & Hasimoto (1980) and Liron & Shahar (1978), when the latter are specialized to source point on the axis. The relation of the function $M(q)$ to the function $D_1(q)$ of Liron & Shahar is $M(q) = qD_1(q)$.

From (2.22), we find for the steady state pressure

$$p_{10}(\boldsymbol{r}) = \frac{P}{\pi^2}\,\mathrm{e}^{\mathrm{i}\varphi}\int_0^\infty A_2(k)kI_1(kR)\cos kz\,\mathrm{d}k. \tag{3.8}$$

In figure 1, we show the behaviour of the normalized steady-state pressure disturbance $4\pi p_0(\boldsymbol{r})/P$ for $x = 0.5b$, $y = 0$ and impulse $\boldsymbol{P} = P\boldsymbol{e}_x$ as a function of z. The decay with z is faster than the behaviour in infinite space given by (3.2). One can check that the flow field $(\boldsymbol{v}_0(\boldsymbol{r}), p_0(\boldsymbol{r}))$ satisfies the steady-state Stokes equations and the no-slip boundary condition.

4. Time-dependent flow

The explicit expressions found above allow the calculation of velocity and pressure at any point $\boldsymbol{r}$ in the tube and at any time t by numerical inversion of the Fourier transform with respect to frequency. The pressure may be written as

$$p(\boldsymbol{r}, t) = p_s + \delta p(\boldsymbol{r}, t), \tag{4.1}$$

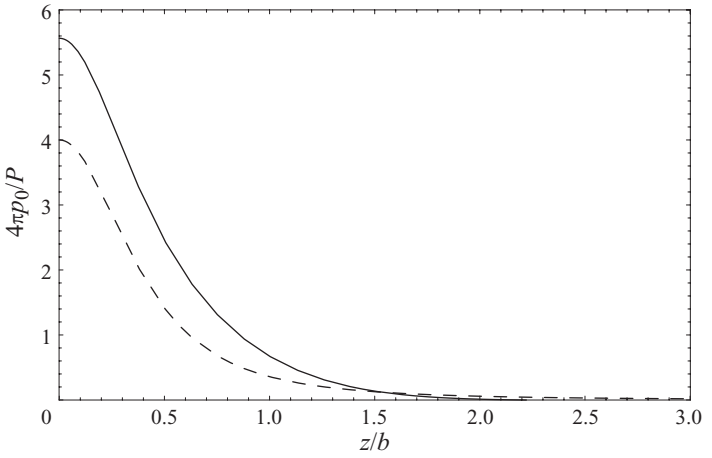

FIGURE 1. Plot of the reduced steady state pressure $4\pi p_0/P$ at $x = 0.5b$, $y = 0$ as a function of z (solid curve). The dashed curve shows the corresponding pressure in infinite space.

where the time dependence of the disturbance δp follows by inverse transform of the expressions in (2.20) and (2.22). In the incompressible limit, a non-vanishing pressure perturbation is established everywhere instantaneously due to the infinite velocity of sound. For a compressible fluid the pressure at any point different from the origin initially equals the static pressure p_s. At later times, a pressure pulse passes through the point. We have found that for the initial impulse parallel to the axis the confinement in the tube causes a slow decay of the pressure disturbance with a $t^{-3/2}$ power law at long times (Felderhof 2009). If the initial impulse is perpendicular to the axis, the decay of pressure is much faster.

For parallel excitation the $t^{-3/2}$ power-law decay of the pressure is caused by coupling to diffusive sound waves. For transverse excitation, there is no such coupling. The function $Z(k, \omega)$ in (2.18) does not have a zero on the negative imaginary ω-axis for small k, unlike the case of parallel excitation.

We consider a compressible fluid with parameters chosen as in the computer simulation of Hagen *et al.* (1997). In their units the mass density ρ_0 is 24, the shear viscosity η is 14.4 and the sound velocity c_0 is $1/\sqrt{2}$. The bulk viscosity $\eta_v = 1/30$ (Frenkel & Lowe 2005 private communication). In figure 2, we show the normalized pressure disturbance $4\pi\delta p/P$ at the chosen point $x = 0.5b$, $y = 0$, $z = 0.5b$ for a tube of radius $b = 1$ as a function of time for initial impulse in the x-direction. We compare with the normalized pressure perturbation $4\pi p_1/P$. It is evident that at long time the pressure disturbance δp is dominated by p_1. We find numerically that the pressure perturbation $p_1(\boldsymbol{r}, t)$ at the fixed point decays at long times at least as fast as with a $t^{-15/2}$ power law. A power-law form of the decay is not assured.

In conclusion, we study the velocity autocorrelation function of a Brownian particle of radius a and mass m_p, initially located at the origin. We consider only the components of the motion transverse to the axis of the tube. The velocity autocorrelation function may be evaluated as the Fourier transform of the transverse components of the frequency-dependent admittance tensor, which gives the mean velocity response of the particle to an applied harmonic force. The admittance tensor differs from that for infinite space because of the no-slip boundary condition at the wall. For $a \ll b$, the difference may be expressed in terms of a reaction field tensor.

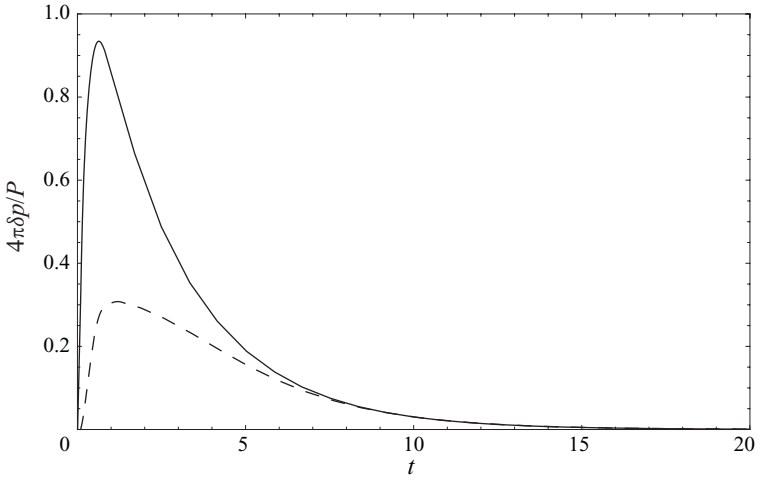

FIGURE 2. Plot of the normalized pressure disturbance $4\pi\delta p/P$ at the point $x = 0.5b$, $y = 0$, $z = 0.5b$ in a tube of radius $b = 1$ in a compressible fluid with properties as in the computer simulation of Hagen *et al.* (1997) as a function of time (solid curve). The dashed curve shows the contribution of the reflected wave $4\pi p_1/P$.

Here we need the complex transverse component given by

$$F_{11}(\mathbf{0}, \omega) = v_{1\omega 1}(\mathbf{0})/P. \tag{4.2}$$

The relevant element of the admittance tensor is (Felderhof 2005)

$$\mathscr{Y}_{11}(\mathbf{0}, \omega) = \mathscr{Y}_0(\omega)\big[1 + A(\omega)C(\omega)F_{11}(\mathbf{0}, \omega)\big], \tag{4.3}$$

where $\mathscr{Y}_0(\omega)$ is the scalar admittance for infinite space. The expressions for $\mathscr{Y}_0(\omega)$ and the coefficients $A(\omega)$ and $C(\omega)$ have been given elsewhere (Felderhof 2009).

The zero-frequency admittance is the particle mobility. The xx-component of the mobility tensor is

$$\mu_{xx}(\mathbf{0}) = \frac{1}{6\pi\eta a}\left(1 - k_0\frac{a}{b}\right). \tag{4.4}$$

From (3.3) we find that the dimensionless coefficient k_0 is

$$k_0 = -\frac{3}{\pi}b\int_0^\infty \left[A_0(k) + \frac{1}{2}kbA_1(k)\right] \mathrm{d}k \tag{4.5}$$

with numerical value $k_0 = 1.80436$, in agreement with Hasimoto's result (Hasimoto 1976). As noted by Hasimoto, it is interesting that the value is less than the value 2.10444 for parallel excitation. This is contrary to what one would expect from the behaviour near a plane wall, as calculated by Lorentz (1907). For a plane wall the coefficient is $9/8$ for transverse excitation and $9/16$ for parallel excitation (Happel & Brenner 1973).

In the theory of Brownian motion, the velocity autocorrelation function of the particle is defined by

$$C_{xx}(t) = \langle U_x(t)U_x(0)\rangle, \tag{4.6}$$

where the angle brackets denote the equilibrium ensemble average. By axial symmetry the correlation function $C_{yy}(t)$ takes the same value, and the cross-correlation $C_{xy}(t)$ vanishes. According to the fluctuation–dissipation theorem the Fourier transform of

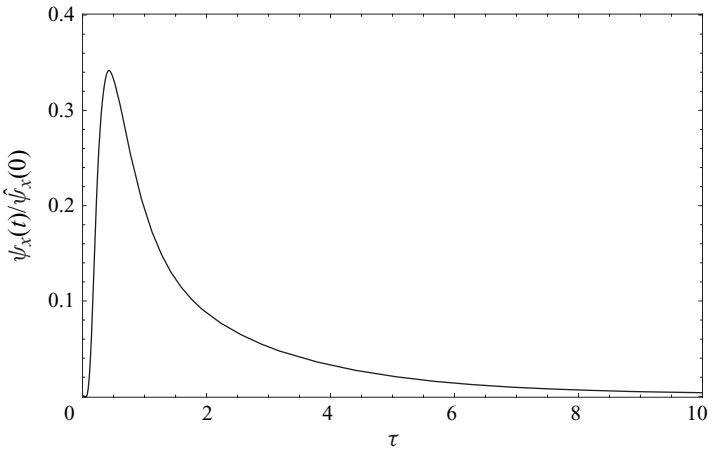

FIGURE 3. Plot of $\psi_x(t)/\hat{\psi}_x(0)$ as a function of τ for the same fluid as in figure 2.

$C_{xx}(t)$ is given by

$$\hat{C}_{xx}(\omega) = \int_0^\infty \mathrm{e}^{\mathrm{i}\omega t} C_{xx}(t)\,\mathrm{d}t = k_B T \mathscr{Y}_{xx}(\mathbf{0}, \omega). \tag{4.7}$$

The reaction factor $F_{xx}(\mathbf{0}, \omega)$ may be regarded as the Fourier transform of a function $\psi_x(t)$ according to

$$F_{xx}(\mathbf{0}, \omega) = \frac{1}{6\pi\rho_0} \int_0^\infty \mathrm{e}^{\mathrm{i}\omega t} \psi_x(t)\,\mathrm{d}t. \tag{4.8}$$

The function $\psi_x(t)$ starts at zero, because the sound wave needs a finite time to be reflected from the wall of the tube. An asymptotic calculation of the integrands in (3.3) shows that as a consequence of the behaviour of the integrands for small k, the function $\psi_x(t)$ decays with a $t^{-3/2}$ long-time tail as

$$\psi_x(t) \approx -\frac{1}{2\sqrt{\pi} b^3} \tau^{-3/2} \qquad \text{as } t \to \infty, \tag{4.9}$$

where $\tau = t/\tau_b$ with $\tau_b = b^2/\nu$. In figure 3, we plot the ratio $\psi_x(t)/\hat{\psi}_x(0)$, where $\hat{\psi}_x(0) = -k_0/(b\nu)$, as a function of τ. In figure 4, we plot the same function on a doubly logarithmic scale.

The product $A(\omega)C(\omega)$ in (4.3) has the low-frequency expansion

$$A(\omega)C(\omega) = 6\pi\eta a(1 + \alpha a) + O(\omega). \tag{4.10}$$

Combining results, we find for the low-frequency expansion of the admittance

$$\mathscr{Y}_{xx}(\mathbf{0}, \omega) = \frac{1}{6\pi\eta a}\left(1 - k_0 \frac{a}{b}\right) + O(\omega) \tag{4.11}$$

with coefficient k_0 given by (4.5). The term linear in α cancels, and this implies that the correlation function decays faster than $t^{-3/2}$ at long times. In figure 5, we plot the normalized velocity autocorrelation function $C_{xx}(t)/C_{xx}(0)$, calculated from (4.7), as a function of τ for a neutrally buoyant particle of radius $a = 5b/9$ in the same fluid as before. The minimum is about twice as deep as for the longitudinal

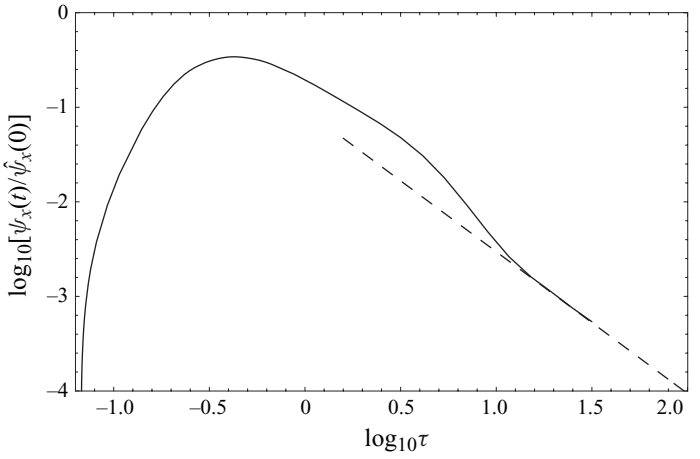

FIGURE 4. Plot of $\log_{10}[\psi_x(t)/\hat{\psi}_x(0)]$ as a function of $\log_{10}\tau$ for the same fluid as in figure 2 (solid curve). We compare with the straight line corresponding to the long-time tail given by (4.9) (dashed line).

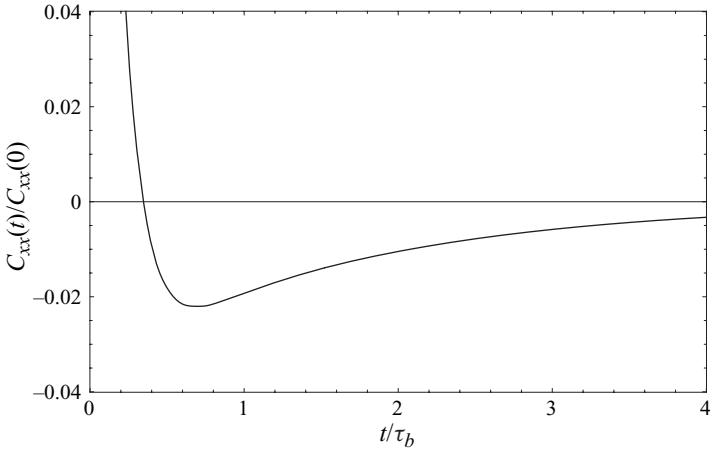

FIGURE 5. Plot of the normalized velocity autocorrelation function $C_{xx}(t)/C_{xx}(0)$ as a function of τ for a neutrally buoyant particle of radius $a = 5b/9$ centred on average at the origin in the same fluid as in figure 2.

correlation function. For this case the longitudinal correlation function was studied in the computer simulation by Hagen *et al.* (1997) and Pagonabarraga *et al.* (1999). In figure 6, we plot the corresponding function $\log_{10}|C_{xx}(t)/C_{xx}(0)|$ as a function of $\log_{10}\tau$. The correlation function appears to decay at least as fast as with a negative $t^{-9/2}$ long-time tail. A power-law form of the decay is not assured. The behaviour is qualitatively different from that found for plane plate geometry in the lattice Boltzmann computer simulation by Frydel & Rice (2006, 2007), where the correlation function was positive with superposed oscillations. For a more compressible fluid in the same geometry the behaviour is more like that seen here; see figures 6 and 8 of Felderhof (2006) (the function plotted in figure 8 is $\gamma_{zz}(t)$, not $\gamma_{xx}(t)$ as indicated erroneously in that paper).

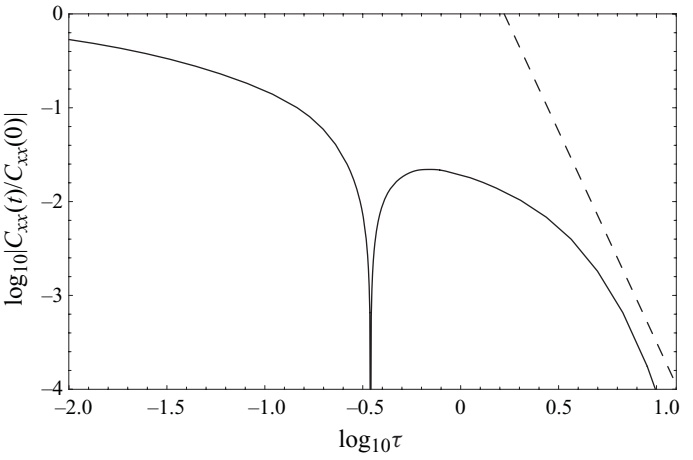

FIGURE 6. Plot of $\log_{10}|C_{xx}(t)/C_{xx}(0)|$ as a function of $\log_{10}\tau$ corresponding to figure 5 (solid curve). The straight line corresponds to a $t^{-9/2}$ power law (dashed line).

5. Discussion

The above calculation completes the calculation of the Green function for the flow of a compressible viscous fluid confined in a circular tube with the restriction that the source point is located on the axis of the tube. It turns out that the flow for transverse excitation differs qualitatively from that for parallel excitation. For transverse excitation there is no coupling to diffusive sound waves, and the flow velocity decays at long times fast in comparison with parallel excitation. The time dependence of both flows is strongly affected by compressibility. The integral over all time is independent of compressibility and given by the solution of the steady-state Stokes equations for an incompressible fluid.

Although the restriction of the source point to the axis of the tube is somewhat special, it has the advantage of significant simplification compared to the general case. The Green function can be used in interesting applications.

REFERENCES

FELDERHOF, B. U. 2005 Effect of the wall on the velocity autocorrelation function and long-time tail of Brownian motion in a viscous compressible fluid. *J. Chem. Phys.* **123**, 184903.

FELDERHOF, B. U. 2006 Diffusion and velocity relaxation of a Brownian particle immersed in a viscous compressible fluid confined between two parallel plane walls. *J. Chem. Phys.* **124**, 054111.

FELDERHOF, B. U. 2009 Transient flow of a viscous compressible fluid in a circular tube after a sudden point impulse. *J. Fluid Mech.* **603**, 285.

FRYDEL, D. & RICE, S. A. 2006 Lattice Boltzmann study of the transition from quasi-two-dimensional to three-dimensional one particle hydrodynamics. *Mol. Phys.* **104**, 1283.

FRYDEL, D. & RICE, S. A. 2007 Hydrodynamic description of the long-time tails of the linear and rotational velocity autocorrelation functions of a particle in a confined geometry. *Phys. Rev.* E **76**, 061404.

GRADSHTEYN, I. S. & RYZHIK, I. M. 1965 *Table of Integrals, Series and Products*. Academic Press.

HAGEN, M. H. J., PAGONABARRAGA, I., LOWE, C. P. & FRENKEL, D. 1997 Algebraic decay of velocity fluctuations in a confined fluid. *Phys. Rev. Lett.* **78**, 3785.

HAPPEL, J. & BRENNER, H. 1973 *Low Reynolds Number Hydrodynamics*. Noordhoff.

Hasimoto, H. 1976 Slow motion of a small sphere in a cylindrical domain. *J. Phys. Soc. Japan* **41**, 2143.

Ishii, K. & Hasimoto, H. 1980 Lateral migration of a spherical particle in flows in a circular tube. *J. Phys. Soc. Japan* **48**, 2144.

Jones, R. B. 1981 Hydrodynamic fluctuation forces. *Physica* A **105**, 395.

Liron, N. & Shahar, R. 1978 Stokes flow due to a Stokeslet in a pipe. *J. Fluid Mech.* **78**, 727.

Lorentz, H. A. 1907 Ein allgemeiner Satz, die Bewegung einer reibenden Flüssigkeit betreffend, nebst einigen Anwendungen desselben. In *Abhandlungen über theoretische Physik*, p. 23. Teubner.

Pagonabarraga, I., Hagen, M. H. J., Lowe, C. P. & Frenkel, D. 1999 Short-time dynamics of colloidal suspensions in confined geometries. *Phys. Rev.* E **59**, 4458.